

Isolating Sources of Disentanglement in Variational Autoencoders

Tian Qi Chen^{1,2} Xuechen Li^{1,2} Roger Grosse^{1,2} David Duvenaud^{1,2}

Abstract

We decompose the evidence lower bound to show the existence of a term measuring the total correlation between latent variables. We use this to motivate our β -TCVAE (Total Correlation Variational Autoencoder), a refinement of the state-of-the-art β -VAE objective for learning disentangled representations, requiring no additional hyperparameters during training. We further propose a principled classifier-free measure of disentanglement called the mutual information gap (MIG). We perform extensive quantitative and qualitative experiments, in both restricted and non-restricted settings, and show a strong relation between total correlation and disentanglement, when the latent variables model is trained using our framework.

1. Introduction

Learning disentangled representations without supervision is a difficult open problem. Disentangled variables are generally considered to contain a combination of interpretable semantic information and the ability to independently act on the generative process. While the proper expression for disentanglement is a subject of philosophical debate, many believe a factorial representation, one with statistically independent variables, is a good starting point (Schmidhuber, 1992; Ridgeway, 2016; Achille & Soatto, 2017). Such a representation distills information into a compact form which is oftentimes semantically meaningful and useful for a variety of tasks (Ridgeway, 2016; Bengio et al., 2013). For instance, (Alemi et al., 2017a) have found such representations to be more generalizable and robust against adversarial attacks.

Many state-of-the-art methods for learning disentangled representations are based on increasing the penalty on parts of an existing objective. For instance, Chen et al. (2016) claim that mutual information between the latent variables and observed data can encourage the latent variables into becoming more interpretable. Tangentially, Higgins et al.

¹University of Toronto ²Vector Institute. Correspondence to: Tian Qi (Ricky) Chen <rtqichen@cs.toronto.edu>.

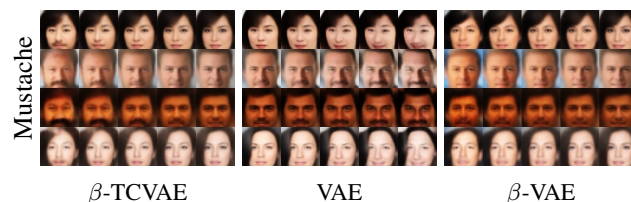


Figure 1. A β -TCVAE model can use a single latent variable to represent mustache while a VAE’s latent variable is entangled with smiling, but a β -VAE model fails to discover this attribute.

(2017) believes that encouraging independence in latent variables causes disentanglement. However, there is no strong evidence linking factorial representations to disentanglement. In part this can be attributed to the problems of the evaluation procedure itself. While traversals in the latent representation can illustrate disentanglement qualitatively, proper statistical measures of disentanglement can show subtle differences in models and robustness to hyperparameter settings.

We contribute to the learning of disentangled representations by first showing that a widely used objective for learning representations, the evidence lower bound, can be rewritten to contain terms describing both independence of the latent variables and the mutual information between latent variables and the observed data (Section 3). Based on this, we analyze the β -VAE objective (Higgins et al., 2017) and propose an improved β -TCVAE that requires no additional hyperparameters during training. To evaluate our method, we propose mutual information gap (MIG), a principled information-theoretic quantity that measures disentanglement (Section 4). Compared to β -VAE, we find that β -TCVAE is more reliable, can discover more features, and exhibit stronger correlation between factorial and disentangled representations (Section 6).

2. Background

We discuss existing works that aim at either learning disentangled representations without supervision or evaluating such learned representations. The two problems are inherently related, since improvements to learning algorithms require evaluation metrics that are sensitive to subtle details, and stronger evaluation metrics reveal deficiencies in

existing methods.

2.1. Learning Disentangled Representations

Variational Autoencoder The variational autoencoder (VAE) (Kingma & Welling, 2013) is a latent variable model that pairs a top-down generative model with a bottom-up inference network. Instead of directly performing maximum likelihood estimation on the intractable marginal log-likelihood, training is done by optimizing the tractable *evidence lower bound* (ELBO). We would like to optimize this lower bound averaged over the empirical distribution:

$$\mathcal{L}_{\text{ELBO}}^{\text{avg}} = \frac{1}{N} \sum_{n=1}^N (\mathbb{E}_q[\log p(x_n|z)] - \text{D}_{\text{KL}}(q(z|x_n)||p(z))). \quad (1)$$

where the decoder $p(x_n|z)$ and encoder $q(z|x_n)$ are parameterized by deep neural networks. For certain families of distributions, the gradients can be estimated using the *reparameterization trick*. Kingma & Welling (2013) additionally show that a properly trained VAE can disentangle emotion and pose of simple face images in the latent manifold.

β -VAE The β -VAE (Higgins et al., 2017) is a variant of the variational autoencoder that attempts to learn a disentangled representation by optimizing a heavily penalized objective:

$$\mathcal{L}_{\beta} = \frac{1}{N} \sum_{n=1}^N (\mathbb{E}_q[\log p(x_n|z)] - \beta \text{D}_{\text{KL}}(q(z|x_n)||p(z))) \quad (2)$$

where $\beta > 1$. Higgins et al. (2017) argue that if $p(z)$ is factorial then the latent representations will also be encouraged to become independent. Such simple penalization has been shown to be capable of obtaining models with a high degree of disentanglement in image datasets. However, it isn't made explicit why penalizing $\text{D}_{\text{KL}}(q(z|x)||p(z))$ with a factorial prior can lead to learning latent variables that exhibit disentangled transformations for all data samples.

InfoGAN The InfoGAN (Chen et al., 2016) is a variant of the generative adversarial network (GAN) (Goodfellow et al., 2014) that encourages an interpretable latent representation by maximizing the mutual information between the observation and a small subset of latent variables. The approach relies on optimizing a lower bound of the intractable mutual information.

2.2. Evaluating Disentangled Representations

When the true underlying generative factors are known and we have reason to believe that this set of factors is disentangled, then it is possible to create a supervised evaluation metric. Many have proposed classifier-based metrics

for assessing the quality of disentanglement (Grathwohl & Wilson, 2016; Higgins et al., 2017; Kim & Mnih, 2017; Cian Eastwood, 2018; Glorot et al., 2011; Karaletsos et al., 2016). We focus on discussing the metrics proposed by Higgins et al. (2017) and Kim & Mnih (2017) as they are relatively simple in design and generalizable.

The Higgins et al. (2017) metric is defined as the accuracy that a low VC-dimension linear classifier can achieve at identifying a fixed ground truth factor. Specifically, for a set of ground truth factors $\{v_k\}_{k=1}^K$, each training data point is an aggregation over L samples: $\frac{1}{L} \sum_{l=1}^L |z_l^{(1)} - z_l^{(2)}|$, where random vectors $z_l^{(1)}, z_l^{(2)}$ are drawn i.i.d. from $q(z|v_k)$ ¹ for any fixed value of v_k , and a classification target k . A drawback of this method is the lack of axis-alignment detection. That is, we believe a truly disentangled model should only contain one latent variable that is related to each factor. As a means to include axis-alignment detection, Kim & Mnih (2017) proposes using $\text{argmin}_j \text{Var}_{q(z|v_k)}(z_j)$ and a majority-vote classifier.

Classifier-based disentanglement metrics tend to be ad hoc and can produce varying results depending on hyperparameters. Both the Higgins et al. (2017) and Kim & Mnih (2017) metrics can be loosely interpreted as measuring the reduction in entropy of z if v is observed. In section 4, we show that it is possible to directly measure the mutual information between z and v which is a principled information-theoretic quantity that can be used for any latent distributions provided that efficient estimation exists.

3. Sources of Disentanglement in the ELBO

As evidenced by Chen et al. (2016) and Higgins et al. (2017), we have reason to conjecture that the following two criteria may be of importance in learning a disentangled representation:

- (i) Mutual information between the latent variables and the data variable.
- (ii) Independence between the latent variables.

Hoffman & Johnson (2016) analyzed an ELBO decomposition, showcasing a term that quantifies criterion (i). In this section, we introduce a refined decomposition showing that terms describing both criteria appear in the ELBO.

3.1. ELBO TC-Decomposition

Following the notation in the decomposition by Hoffman & Johnson (2016), we identify each training example with a unique integer index and define a uniform random variable on $\{1, 2, \dots, N\}$ with which we relate to

¹Note that $q(z|v_k)$ is sampled by using an intermediate data sample: $z \sim q(z|x), x \sim p(x|v_k)$.

$$\mathbb{E}_{p(n)} \left[\text{D}_{\text{KL}}(q(z|n) \| p(z)) \right] = \underbrace{\text{D}_{\text{KL}}(q(z, n) \| q(z)p(n))}_{\text{(i) Index-Code MI}} + \underbrace{\text{D}_{\text{KL}}(q(z) \| \prod_j q(z_j))}_{\text{(ii) Total Correlation}} + \underbrace{\sum_j \text{D}_{\text{KL}}(q(z_j) \| p(z_j))}_{\text{(iii) Dimension-wise KL}} \quad (3)$$

data points. Furthermore, we define $q(z|n) = q(z|x_n)$ and $q(z, n) = q(z|n)p(n) = q(z|n)\frac{1}{N}$. We refer to $q(z) = \sum_{n=1}^N q(z|n)p(n)$ as the *aggregated posterior* following Makhzani et al. (2016). With such notation, we decompose the KL term in (1) assuming a factorized $p(z)$. The decomposition is shown in (3) where z_j denotes the j th dimension of the latent variable (see Supplementary Materials for derivation).

3.1.1. DECOMPOSITION ANALYSIS

In a similar decomposition, Hoffman & Johnson (2016) refer to (i) as the *index-code mutual information* (MI). The index-code MI is the mutual information $I_q(z; n)$ between the data variable and latent variable based on the empirical data distribution $q(z, n)$. In fact, (i) can be viewed as a consistent but biased estimator for the mutual information between $p(x)$ and $q(z)$ under the true data generating distribution, as the expectation of the index-code MI is a lower bound. Since $p(n)$ here is the empirical data distribution, the subtlety is that a higher index-code MI would imply the latent variables have sufficient information for distinguishing the empirical samples. Chen et al. (2016) have argued that a higher mutual information can lead to disentanglement, and some have even proposed completely disregarding this term (Makhzani et al., 2016; Zhao et al., 2017).

In information theory, (ii) is referred to as the *total correlation* (TC), one of many generalizations of mutual information to more than two random variables (Watanabe, 1960). The naming is unfortunate as it is actually a measure of dependence between the variables. We argue that a heavier penalty on this term induces a more disentangled representation, since intuitively, this KL term measures the difference between the actual joint distribution of the aggregate posterior and the ideal factorized joint.

We refer to (iii) as the *dimension-wise KL*. This term mainly prevents the individual latent dimensions from deviating too far from their corresponding priors. It acts as a complexity penalty on the aggregate posterior which reasonably follows from the minimum description length (Hinton & Zemel, 1994) formulation of the ELBO.

3.1.2. ANALYZING THE β -VAE

Recall that the β -VAE increases the penalty on the average-of-KL's term in the vanilla ELBO. In the context of our

decomposition, this corresponds to increasing the weight on all three terms. More specifically, this means the objective encourages low total correlation but simultaneously penalizes the index-code mutual information.

We hypothesize that a low total correlation is the main reason β -VAE achieves empirical success in learning disentangled representations. However, more importantly, we should emphasize that because β -VAE penalizes the index-code mutual information by the same weight, it cannot obtain low total correlation without also obtaining a low index-code MI. This encourages the model to discard information from the latent variables, resulting in poor use of the latent variables in the generative model. Such reasoning resonates with the observed behavior that β is a hyperparameter that requires careful tuning and that large β values typically fail in practice (Higgins et al., 2017; Alemi et al., 2017b).

3.2. β -TCVAE

It is possible to assign different penalty weights to the terms in (3), but instead, we propose a simple alternative to the β -VAE objective and penalize only the total correlation term. We do not further penalize the index-code MI since we are interested in obtaining a useful latent-variable model. Moreover, neither do we further penalize the dimension-wise KL as we do not believe it is interesting for learning disentangled representations.

$$\begin{aligned} \mathcal{L}_{\beta\text{-TC}} := & \frac{1}{N} \sum_{n=1}^N (\mathbb{E}_{q(z|n)} [\log p(n|z)]) - I_q(z; n) \\ & - \beta \text{D}_{\text{KL}}(q(z) \| \prod_j q(z_j)) \\ & - \sum_j \text{D}_{\text{KL}}(q(z_j) \| p(z_j)) \end{aligned} \quad (4)$$

where $\beta > 1$. This allows us to train latent-variable models that encourage an independent aggregated posterior, which should increase the chances of obtaining a disentangled representation. Note that different penalization coefficients can be used for all terms in the decomposition, but we keep the other coefficients at one to ensure a valid lower bound on the likelihood.

3.2.1. TRAINING WITH MINIBATCH IMPORTANCE SAMPLING

The decomposed expression (3) requires the evaluation of $q(z) = \mathbb{E}_{p(n)}[q(z|n)]$, which depends on the entire empirical dataset. As such, it is undesirable to compute it exactly during training. We discuss one possible way to estimate this stochastically using a minibatch of samples without any added hyperparameters.²

First notice that a naïve Monte Carlo approximation based on a minibatch of samples from $p(n)$ is very likely to underestimate $q(z)$. This can be intuitively seen by viewing $q(z)$ as a mixture distribution where the data index n indicates the mixture component. With a randomly sampled component, $q(z|n)$ is close to 0, whereas $q(z|n)$ would be large if n is the component that z came from. So it is much better to sample this component and weight the probability appropriately.

To this end, we propose using a minibatch importance sampled version for estimating the function $\log q(z)$ during training. When provided with a minibatch of samples $\{n_1, \dots, n_M\}$, we can use the estimator

$$\mathbb{E}_{q(z)}[\log q(z)] \approx \frac{1}{M} \sum_{i=1}^M \left[\log \frac{1}{NM} \sum_{j=1}^M q(z(n_i)|n_j) \right] \quad (5)$$

where $z(n_i)$ is a sample from $q(z|n_i)$ (see derivation in Supplementary Materials).

Note that while this minibatch estimator is consistent as $M \rightarrow \infty$ and has low variance, it is biased since its expectation is a lower bound³. Despite this bias, we note that this trick is crucial for enabling training, and may be advantageous due to the absence of any additional hyperparameters compared to methods that require training auxiliary neural nets (Kim & Mnih, 2017; Zhao et al., 2017).

4. Measuring Disentanglement with MIG

It is difficult to compare disentangling algorithms without a proper metric. Most prior works have resorted to visualizing the effects of change in the representation. This is tedious and cannot be used to measure the robustness of an approach. Furthermore, a metric should itself be robust to hyperparameters so that properties of robustness (or lack thereof) can be properly attributed to the algorithm. Existing classifier-based metrics use simple classifier to reduce the amount of variance, but the necessity of designing a dataset is not hyperparameter-free and can bias the metric value

²The same argument holds for the term $\prod_j q(z_j)$ and a similar estimator can be constructed.

³This follows from Jensen’s inequality $\mathbb{E}_{p(n)}[\log q(z|n)] \leq \log \mathbb{E}_{p(n)}[q(z|n)]$.

Disentanglement Metric	Axis	Unbiased	General
Higgins et al. (2017)	No	No	No
Kim & Mnih (2017)	Yes	No	No
MIG (Ours)	Yes	Yes	Yes

Table 1. In comparison to prior metrics, our proposed MIG detects axis-alignment, is unbiased for all hyperparameter settings, and can be generally applied to any latent distributions provided efficient estimation exists.

(see Supplementary Materials).

We can measure a notion of disentanglement when the empirical generative process $p(n|v)$ and its ground truth latent factors v are known. Often these are semantically meaningful scalar attributes of the data sample. For instance, photographic portraits generally contain disentangled factors such as pose (azimuth and elevation), lighting condition, and attributes of the face such as skin tone, gender, face width, etc. Though not all ground truth factors may be provided, it is still possible to evaluate disentanglement using the known factors. To this end, we propose a metric based on the empirical mutual information between latent variables and ground truth factors.

4.1. Mutual Information Gap (MIG)

Our key insight is that the *empirical mutual information* between a latent variable z_j and a ground truth factor v_k can be estimated using the joint distribution defined by $q(z_j, v_k) = \mathbb{E}_{p(n)}[p(v_k)p(n|v_k)q(z_j|n)]$. Assuming that the underlying factors $p(v_k)$ and the generating process is known for the empirical data samples $p(n|v_k)$, then

$$I_n(z_j; v_k) = \mathbb{E}_{p(v_k, z_j)} \left[\log \sum_{n \in \mathcal{X}_{v_k}} q(z_j|n)p(n|v_k) \right] + H(z_j) \quad (6)$$

where \mathcal{X}_{v_k} is the support of $p(n|v_k)$. (See derivation in Supplementary Materials.)

The mutual information is an information-theoretic quantity able to describe the relationship between z_j and v_k regardless of their parameterization. A higher mutual information implies that z_j contains a lot of information about v_k , and the mutual information is maximal if there exists an invertible relationship between z_j and v_j . Furthermore, for quantized v_k , the mutual information is bounded $0 \leq I(z_j; v_k) \leq H(v_k)$, where $H(v_k) = \mathbb{E}_{p(v_k)}[-\log p(v_k)]$ is the entropy of v_k . As such, we use the normalized mutual information $I(z_j; v_k)/H(v_k)$.

Note that a single factor can have high mutual information with multiple latent variables. We enforce an axis-alignment

detection by measuring the difference between the top two latent variables with highest mutual information. The full metric we call *mutual information gap* (MIG) is then

$$\frac{1}{K} \sum_{k=1}^K \frac{1}{H(v_k)} \left(I_n(z_{j^{(k)}}; v_k) - \max_{j \neq j^{(k)}} I_n(z_j; v_k) \right) \quad (7)$$

where $j^{(k)} = \operatorname{argmax}_j I_n(z_j; v_k)$ and K is the number of known factors. MIG is bounded between 0 and 1.

While it is possible to compute just the average maximal MI, $\frac{1}{K} \sum_{k=1}^K \frac{I_n(z_{k^*}; v_k)}{H(v_k)}$, the gap in our formulation (7) defends against two important cases. The first case is related to rotation of the factors. When a set of latent variables are not axis-aligned, each variable can contain a decent amount of information regarding two or more factors. The gap heavily penalizes unaligned variables, which is an indication of entanglement. The second case is related to compactness of the representation. If one latent variable reliably models a ground truth factor, then it is unnecessary for other latent variables to also be informative about this factor.

As summarized in Table 1, our metric detects axis-alignment and is generally applicable and meaningful for any factorized latent distribution, including vectors of multimodal, Categorical, and other structured distributions. This is because the metric is only limited by whether the mutual information can be estimated. Efficient estimation of mutual information is an ongoing research topic (Belghazi et al., 2018; Reshef et al., 2011), but we find that the simple estimator (6) is sufficient for the datasets we use. We find that MIG can better capture subtle differences in models compared to existing metrics. Systematic experiments analyzing MIG and existing metrics are placed in the Supplementary Materials.

5. Related Work

We focus on discussing the learning of disentangled representations in an unsupervised manner. Nevertheless, we note that inverting generative processes with known disentangled factors through weak supervision has been pursued by many. The goal in this case is not perfect inversion but to distill into a simpler representation (Hinton et al., 2011; Kulkarni et al., 2015; Cheung et al., 2014; Karaletsos et al., 2016; Vedantam et al., 2018). Although not explicitly the main motivation, many unsupervised generative modeling frameworks have explored the disentanglement of their learned representations (Kingma & Welling, 2013; Makhzani et al., 2016; Radford et al., 2015). Prior to β -VAE (Higgins et al., 2017), some have shown successful disentanglement in limited settings with few factors of variation (Schmidhuber, 1992; Tang et al., 2013; Desjardins et al., 2012; Glorot et al., 2011).

With recent progress in generative modeling, Chen et al.

Dataset	Ground truth factors
dSprites	scale (6), rotation (40), posX (32), posY (32)
3D Faces	azimuth (21), elevation (11), lighting (11)

Table 2. Summary of datasets with known ground truth factors. Parentheses contain number of quantized values for each factor.

(2016) propose the InfoGAN by modifying the generative adversarial networks objective (Goodfellow et al., 2014) to encourage high mutual information between a small subset of latent variables and the observed data. This motivates the removal of the index-code MI term in (3) which is explored in some recent works (Makhzani et al., 2016; Kumar et al., 2017; Zhao et al., 2017). However, investigations into generative modeling also claim that a penalized mutual information through the information bottleneck encourages compact and disentangled representations (Achille & Soatto, 2017; Burgess et al., 2017).

As a means to describe the properties of disentangled representations, factorial representations have been motivated by many (Schmidhuber, 1992; Ridgeway, 2016; Achille & Soatto, 2018; Ver Steeg & Galstyan, 2015), where sometimes total correlation is even equated as a measurement of disentanglement. In a similar vein, non-linear independent component analysis (Comon, 1994; Hyvärinen & Pajunen, 1999; Jutten & Karhunen, 2003) studies the problem of inverting a generative process assuming independent latent factors. Instead of a perfect inversion, we only aim for maximizing the mutual information between our learned representation and the ground truth factors. Simple priors can further encourage interpretability by means of warping complex factors into simpler manifolds. Very recently, Kim & Mnih (2017) have also explored penalizing the total correlation in a variational autoencoder; however, we explicitly acknowledge the existence of this term already in the ELBO for factorial priors. Furthermore, our minibatch importance sampling allows adding arbitrary weights to each term in the decomposition (3) and does not require any additional hyperparameters, whereas the learning algorithm by Kim & Mnih (2017) requires an auxiliary discriminator network to estimate the total correlation term. To the best of our knowledge, we are the first to show a strong relation between factorial representations and disentanglement (see Section 6.1.3).

6. Experiments

We perform a series of quantitative and qualitative experiments, showing that β -TCVAE can consistently achieve higher MIG scores compared to two of the state-of-the-art methods, β -VAE and InfoGAN. Furthermore, we find that in

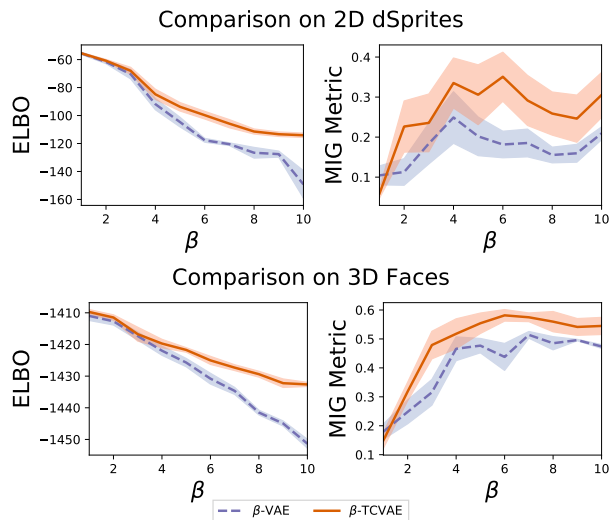


Figure 2. Compared to β -VAE, β -TCVAE creates more disentangled representations while preserving a better generative model of the data with increasing β . Shaded regions show the 90% confidence intervals. Higher is better on both metrics.

models trained with our method, total correlation is strongly correlated with disentanglement.

6.1. Independent Factors of Variation

First, we analyze the performance of our proposed β -TCVAE and MIG metric in a restricted setting, with ground truth factors that are uniformly and independently sampled. To paint a clearer picture on the robustness of learning algorithms, we aggregate results from multiple experiments to visualize the effect of initialization. Adam (Kingma & Ba, 2015) with a learning rate of 0.001 is used to train all models.

We perform quantitative evaluations with two datasets, a dataset of 2D shapes (Matthey et al., 2017) and a dataset of synthetic 3D faces (Paysan et al., 2009). Their ground truth factors are summarized in Table 2. The dSprites and 3D faces also contain 3 types of shapes and 50 identities, respectively, which are treated as noise during evaluation.

6.1.1. ELBO vs. DISENTANGLEMENT TRADE-OFF

Since the β -VAE and β -TCVAE objectives are lower bounds on the standard ELBO, we would like to see the effect of training with this modification. To see how the choice of β affects these learning algorithms, we train using a range of values. The trade-off between density estimation and the amount of disentanglement measured by MIG is shown in Figure 2.

We find that β -TCVAE provides a better trade-off between density estimation and disentanglement. Notably, with

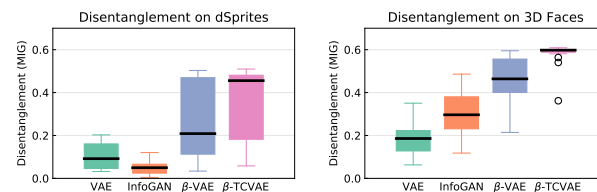


Figure 3. Distribution of disentanglement score (MIG) for different modeling algorithms.

higher values of β , the mutual information penalty in β -VAE is too strong and this hinders the usefulness of the latent variables. However, β -TCVAE with higher values of β consistently results in models with higher disentanglement score relative to β -VAE.

6.1.2. QUANTITATIVE COMPARISONS

While a disentangled representation may be achievable by some learning algorithms, the chances of obtaining such a representation typically isn't clear. Unsupervised learning of a disentangled representation can have high variance since disentangled labels are not provided during training. To further understand the robustness of each algorithm, we show box plots depicting the quartiles of the MIG score distribution for various methods in Figure 3. We used $\beta = 4$ for β -VAE and $\beta = 6$ for β -TCVAE, based on modes in Figure 2. For InfoGAN, we used 5 continuous latent codes and 5 noise variables. Other settings are chosen following those suggested by Chen et al. (2016), but we also added instance noise (Sønderby et al., 2017) to stabilize training.

Despite our best efforts, we were unable to train InfoGAN to disentangle the dSprites dataset. This is likely due to pixels of input images only take on binary values in $\{0, 1\}$, which required the instance noise trick to even train. In general, we find that the median score is highest for β -TCVAE and it is close to the highest score achieved by all methods. Despite the best half of the β -TCVAE runs achieving high scores, we see that the other half can still perform poorly. On modeling 3D faces with β -TCVAE, we see that there exist low-score outliers, although their scores are still higher than the median score achieved by both VAE and InfoGAN.

6.1.3. FACTORIAL vs. DISENTANGLED REPRESENTATIONS

While a low total correlation has been previously conjectured to lead to disentanglement, we provide concrete evidence that our β -TCVAE learning algorithm satisfies this property. Figure 4 shows a scatter plot of total correlation and the MIG disentanglement metric for varying values of β trained on the dSprites and faces datasets, averaged over 40 random initializations. For models trained with β -TCVAE, the correlation between average TC and average

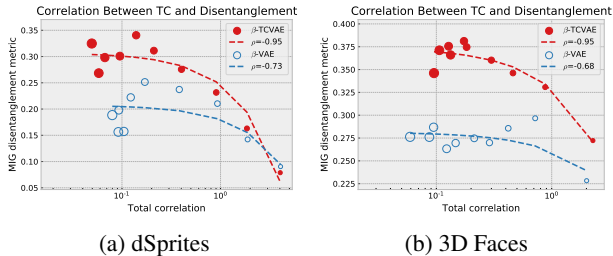


Figure 4. Scatter plots of the average MIG and TC per value of β . Larger circles indicate a higher β . On average, β -TCVAE makes better use of low total correlation scores to reach higher disentanglement. Note the log-scale for TC, though the Pearson correlation coefficients ρ are estimated without using log.

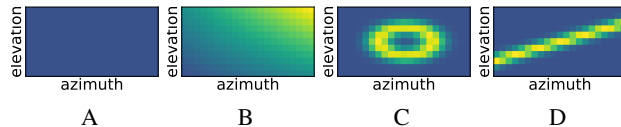
MIG is -0.95 , while models trained with β -VAE have a lower correlation. For the dSprites data, we see that with higher values of β , β -VAE seems to stop decreasing the TC among latent variables while disentanglement further decreases. Meanwhile, β -VAE achieves a lower total correlation than β -TCVAE on the 3D faces dataset, possibly an indication of latent variables regressing towards the prior and becoming inactive. In general, for the same degree of total correlation, β -TCVAE creates a better disentangled model. This is also strong evidence for our hypothesis of β -VAE that large values of β decreases the index-code mutual information in the latent variables, leading to a worse generative model without increased chances of learning a disentangled representation.

6.2. Correlated or Dependent Factors

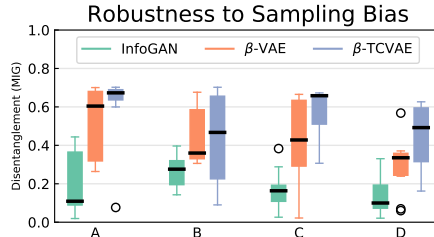
A notion of disentanglement can exist even when the underlying generative process samples factors non-uniformly and dependently. Many real datasets exhibit this behavior, where some configurations of factors are sampled more than others, violating the statistical independence assumption. Disentangling the factors of variation in this case corresponds to finding the generative model where the latent factors can independently act and perturb the generated result, even when there is bias in the sampling procedure. In general, we find that β -TCVAE has no problem in finding the correct factors of variation in a toy dataset and can find more interpretable factors of variation than those found in prior work, even though the independence assumption is violated.

6.2.1. 2D FACTORS

We start off with a toy dataset with only two factors and test β -TCVAE using sampling distributions with varying degrees of correlation and dependence. We take the dataset of synthetic 3D faces and fix the lighting factor. The joint distributions over factors that we test with are summarized in Figure 5a, which includes varying degrees of sampling



(a) Different joint distributions of factors.



(b) Distribution of disentanglement scores (MIG).

Figure 5. The β -TCVAE has a higher chance of obtaining a disentangled representation than β -VAE, even in the presence of sampling bias. (a) All samples have non-zero probability in all joint distributions; the most likely sample is 4 times as likely as the least likely sample.

bias. Specifically, configuration A uses uniform and independent factors; B uses factors with non-uniform marginals but are uncorrelated and independent; C uses uncorrelated but dependent factors; and D uses correlated and dependent factors.

For each method, we train 10 models and compute their MIG. Due to the reduction from three to two factors, we find that $\beta = 4$ is enough to give reasonable results for both β -VAE and β -TCVAE. For InfoGAN, we used 2 continuous codes and 8 noise variables. Box plots showing the quartiles for each configuration are shown in Figure 5. While it is possible to train a disentangled model in all configurations, the chances of obtaining one is overall lower when there exist sampling bias. Across all configurations, we see that β -TCVAE is superior to β -VAE and InfoGAN, and there is a large difference in median scores for most configurations.

6.2.2. QUALITATIVE COMPARISONS

We find that β -TCVAE can discover more disentangled factors on datasets of chairs (Aubry et al., 2014) and real faces (Liu et al., 2015). We qualitatively compare traversals in the latent space.

3D Chairs Figure 6 shows traversals in latent variables that depict an interpretable property in generating 3D chairs. The β -VAE (Higgins et al., 2017) has shown to be capable of learning the first four properties: azimuth, size, leg style, and backrest. However, the leg style change learned by β -VAE does not seem to be consistent for all chairs. We find that β -TCVAE can learn two additional interpretable

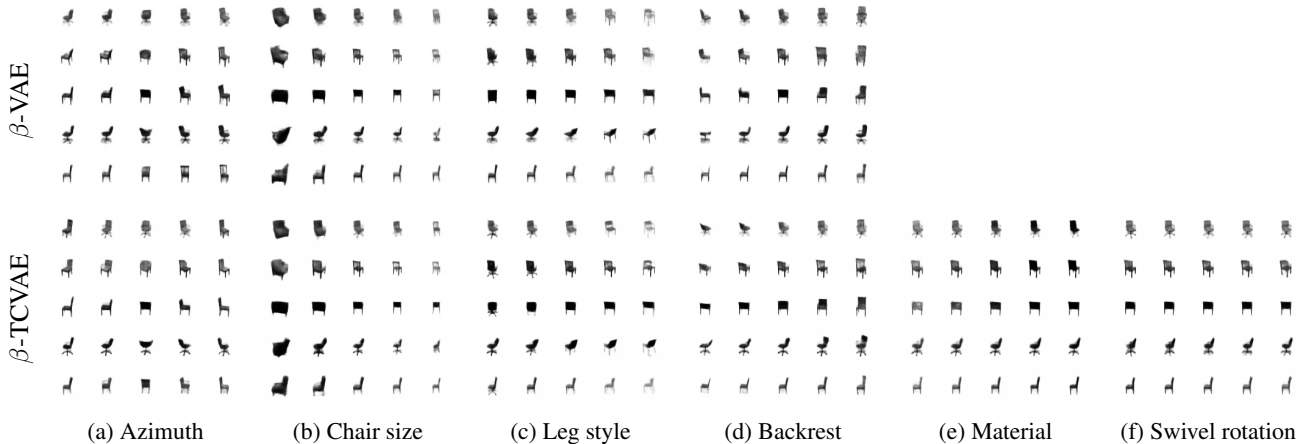


Figure 6. Learned latent variables using β -VAE and β -TCVAE are shown. Traversal range is $(-2, 2)$.

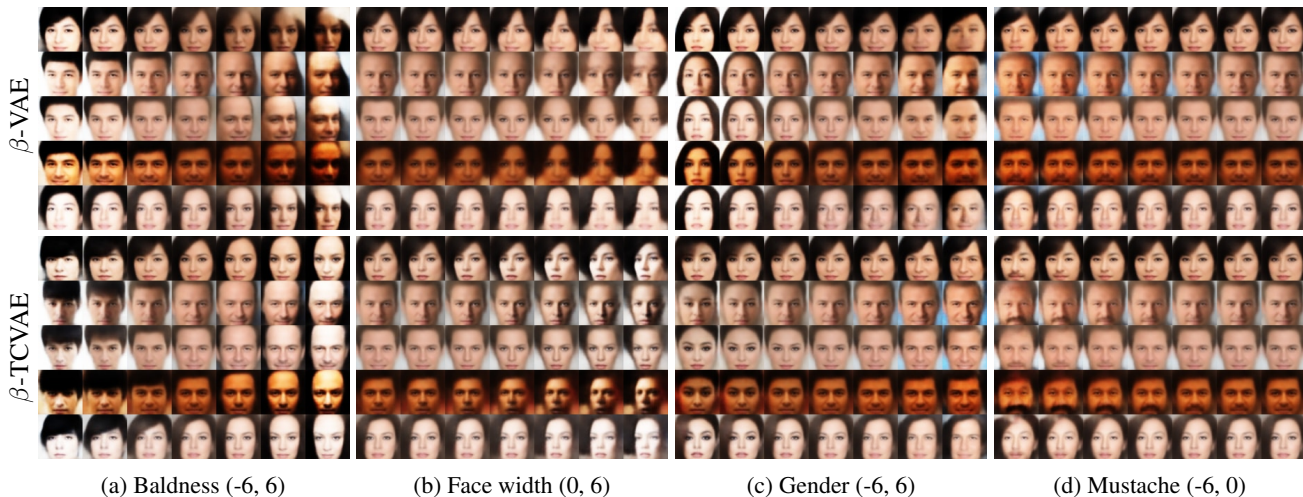


Figure 7. Qualitative comparisons on CelebA. Traversal ranges are shown in parentheses. Some attributes are only manifested in one direction of a latent variable, so we show a one-sided traversal. Most semantically similar variables from a β -VAE are shown for comparison.

properties: material of the chair, and leg rotation for swivel chairs. These two properties are more subtle and likely require a higher index-code mutual information, so the lower penalization of index-code MI in β -TCVAE helps in finding these properties.

CelebA Figure 7 shows 4 out of more than 10 attributes that are discovered by the β -TCVAE without supervision (see more in Supplementary Materials). We traverse in a large range to show the effect of generalizing the represented semantics of each variable. The representation learned by β -VAE is entangled with nuances, which can be shown when generalizing to low probability regions. For instance, it has difficulty rendering complete baldness or narrow face width, whereas the β -TCVAE shows meaningful extrapolation. The extrapolation of the gender attribute

of β -TCVAE shows that it focuses more on gender-specific facial features, whereas the β -VAE is entangled with many irrelevances such as face width. The ability to generalize beyond the first few standard deviations of the prior mean implies that the β -TCVAE model can generate rare samples such as *bald or mustached females*.

7. Conclusion

We present a decomposition of the ELBO and propose β -TCVAE, trained stochastically using minibatch importance sampling. To evaluate our approach, we propose a classifier-free disentanglement metric called MIG. We show that β -TCVAE is superior to β -VAE and InfoGAN in learning disentangled representations. In particular, we are able to discover factors that are too subtle for β -VAE.

References

- Achille, Alessandro and Soatto, Stefano. On the emergence of invariance and disentangling in deep representations. *arXiv preprint arXiv:1706.01350*, 2017.
- Achille, Alessandro and Soatto, Stefano. Information dropout: Learning optimal representations through noisy computation. *IEEE Transactions on Pattern Analysis and Machine Intelligence*, 2018.
- Alemi, Alexander A, Fischer, Ian, Dillon, Joshua V, and Murphy, Kevin. Deep variational information bottleneck. *International Conference on Learning Representations*, 2017a.
- Alemi, Alexander A, Poole, Ben, Fischer, Ian, Dillon, Joshua V, Saurous, Rif A, and Murphy, Kevin. An information-theoretic analysis of deep latent-variable models. *arXiv preprint arXiv:1711.00464*, 2017b.
- Aubry, Mathieu, Maturana, Daniel, Efros, Alexei, Russell, Bryan, and Sivic, Josef. Seeing 3d chairs: exemplar part-based 2d-3d alignment using a large dataset of cad models. In *CVPR*, 2014.
- Belghazi, Ishmael, Rajeswar, Sai, Baratin, Aristide, Hjelm, R Devon, and Courville, Aaron. MINE: Mutual information neural estimation. *arXiv preprint arXiv:1801.04062*, 2018.
- Bengio, Yoshua, Courville, Aaron, and Vincent, Pascal. Representation learning: A review and new perspectives. *IEEE transactions on pattern analysis and machine intelligence*, 35(8):1798–1828, 2013.
- Burda, Yuri, Grosse, Roger, and Salakhutdinov, Ruslan. Importance weighted autoencoders. *arXiv preprint arXiv:1509.00519*, 2015.
- Burgess, Christopher, Higgins, Irina, Pal, Arka, Matthey, Loic, Watters, Nick, Desjardins, Guillaume, and Lerchner, Alexander. Understanding disentangling in beta-vae. *Learning Disentangled Representations: From Perception to Control Workshop*, 2017.
- Chen, Xi, Duan, Yan, Houthoofd, Rein, Schulman, John, Sutskever, Ilya, and Abbeel, Pieter. Infogan: Interpretable representation learning by information maximizing generative adversarial nets. In *Advances in Neural Information Processing Systems*, pp. 2172–2180, 2016.
- Cheung, Brian, Livezey, Jesse A, Bansal, Arjun K, and Olshausen, Bruno A. Discovering hidden factors of variation in deep networks. *arXiv preprint arXiv:1412.6583*, 2014.
- Cian Eastwood, Christopher K. I. Williams. A framework for the quantitative evaluation of disentangled representations. *International Conference on Learning Representations*, 2018.
- Comon, Pierre. Independent component analysis, a new concept? *Signal processing*, 36(3):287–314, 1994.
- Desjardins, Guillaume, Courville, Aaron, and Bengio, Yoshua. Disentangling factors of variation via generative entangling. *arXiv preprint arXiv:1210.5474*, 2012.
- Glorot, Xavier, Bordes, Antoine, and Bengio, Yoshua. Domain adaptation for large-scale sentiment classification: A deep learning approach. In *Proceedings of the 28th international conference on machine learning (ICML-11)*, pp. 513–520, 2011.
- Goodfellow, Ian, Pouget-Abadie, Jean, Mirza, Mehdi, Xu, Bing, Warde-Farley, David, Ozair, Sherjil, Courville, Aaron, and Bengio, Yoshua. Generative adversarial nets. In *Advances in neural information processing systems*, pp. 2672–2680, 2014.
- Goroshin, Ross, Mathieu, Michael F, and LeCun, Yann. Learning to linearize under uncertainty. In *Advances in Neural Information Processing Systems*, pp. 1234–1242, 2015.
- Grathwohl, Will and Wilson, Aaron. Disentangling space and time in video with hierarchical variational autoencoders. *arXiv preprint arXiv:1612.04440*, 2016.
- Higgins, Irina, Matthey, Loic, Pal, Arka, Burgess, Christopher, Glorot, Xavier, Botvinick, Matthew, Mohamed, Shakir, and Lerchner, Alexander. beta-vae: Learning basic visual concepts with a constrained variational framework. *International Conference on Learning Representations*, 2017.
- Hinton, Geoffrey E and Zemel, Richard S. Autoencoders, minimum description length and helmholtz free energy. In *Advances in neural information processing systems*, pp. 3–10, 1994.
- Hinton, Geoffrey E, Krizhevsky, Alex, and Wang, Sida D. Transforming auto-encoders. In *International Conference on Artificial Neural Networks*, pp. 44–51. Springer, 2011.
- Hoffman, Matthew D and Johnson, Matthew J. Elbo surgery: yet another way to carve up the variational evidence lower bound. In *Workshop in Advances in Approximate Bayesian Inference, NIPS*, 2016.
- Hyvärinen, Aapo and Pajunen, Petteri. Nonlinear independent component analysis: Existence and uniqueness results. *Neural Networks*, 12(3):429–439, 1999.

- Jutten, Christian and Karhunen, Juha. Advances in nonlinear blind source separation. 2003.
- Karaletsos, Theofanis, Belongie, Serge, and Rätsch, Gunnar. Bayesian representation learning with oracle constraints. *International Conference on Learning Representations*, 2016.
- Kim, Hyunjik and Mnih, Andriy. Disentangling by factorising. *Learning Disentangled Representations: From Perception to Control Workshop*, 2017.
- Kingma, Diederik P and Ba, Jimmy. Adam: A method for stochastic optimization. *International Conference on Learning Representations*, 2015.
- Kingma, Diederik P and Welling, Max. Auto-encoding variational bayes. *arXiv preprint arXiv:1312.6114*, 2013.
- Kulkarni, Tejas D, Whitney, William F, Kohli, Pushmeet, and Tenenbaum, Josh. Deep convolutional inverse graphics network. In *Advances in Neural Information Processing Systems*, pp. 2539–2547, 2015.
- Kumar, Abhishek, Sattigeri, Prasanna, and Balakrishnan, Avinash. Variational inference of disentangled latent concepts from unlabeled observations. *arXiv preprint arXiv:1711.00848*, 2017.
- Liu, Ziwei, Luo, Ping, Wang, Xiaogang, and Tang, Xiaoou. Deep learning face attributes in the wild. In *Proceedings of the IEEE International Conference on Computer Vision*, pp. 3730–3738, 2015.
- Louizos, Christos, Swersky, Kevin, Li, Yujia, Welling, Max, and Zemel, Richard. The variational fair autoencoder. *arXiv preprint arXiv:1511.00830*, 2015.
- Makhzani, Alireza, Shlens, Jonathon, Jaitly, Navdeep, Goodfellow, Ian, and Frey, Brendan. Adversarial autoencoders. *ICLR 2016 Workshop, International Conference on Learning Representations*, 2016.
- Matthey, Loic, Higgins, Irina, Hassabis, Demis, and Lerchner, Alexander. dsprites: Disentanglement testing sprites dataset. <https://github.com/deepmind/dsprites-dataset/>, 2017.
- Paysan, Pascal, Knothe, Reinhard, Amberg, Brian, Romdhani, Sami, and Vetter, Thomas. A 3d face model for pose and illumination invariant face recognition. In *Advanced Video and Signal Based Surveillance, 2009. AVSS'09. Sixth IEEE International Conference on*, pp. 296–301. Ieee, 2009.
- Radford, Alec, Metz, Luke, and Chintala, Soumith. Unsupervised representation learning with deep convolutional generative adversarial networks. *arXiv preprint arXiv:1511.06434*, 2015.
- Reed, Scott, Sohn, Kihyuk, Zhang, Yuting, and Lee, Honglak. Learning to disentangle factors of variation with manifold interaction. In *International Conference on Machine Learning*, pp. 1431–1439, 2014.
- Reshef, David N, Reshef, Yakir A, Finucane, Hilary K, Grossman, Sharon R, McVean, Gilean, Turnbaugh, Peter J, Lander, Eric S, Mitzenmacher, Michael, and Sabeti, Pardis C. Detecting novel associations in large data sets. *science*, 334(6062):1518–1524, 2011.
- Ridgeway, Karl. A survey of inductive biases for factorial representation-learning. *arXiv preprint arXiv:1612.05299*, 2016.
- Schmidhuber, Jürgen. Learning factorial codes by predictability minimization. *Neural Computation*, 4(6):863–879, 1992.
- Siddharth, N, Paige, Brooks, Van de Meent, Jan-Willem, Desmaison, Alban, and Torr, Philip HS. Learning disentangled representations with semi-supervised deep generative models. *Advances in Neural Information Processing Systems*, 2017.
- Sønderby, Casper Kaae, Caballero, Jose, Theis, Lucas, Shi, Wenzhe, and Huszár, Ferenc. Amortised map inference for image super-resolution. *International Conference on Learning Representations*, 2017.
- Tang, Yichuan, Salakhutdinov, Ruslan, and Hinton, Geoffrey. Tensor analyzers. In *International Conference on Machine Learning*, pp. 163–171, 2013.
- Thomas, Valentin, Pondard, Jules, Bengio, Emmanuel, Sarfati, Marc, Beaudoin, Philippe, Meurs, Marie-Jean, Pineau, Joelle, Precup, Doina, and Bengio, Yoshua. Independently controllable features. *arXiv preprint arXiv:1708.01289*, 2017.
- Vedantam, Ramakrishna, Fischer, Ian, Huang, Jonathan, and Murphy, Kevin. Generative models of visually grounded imagination. *International Conference on Learning Representations*, 2018.
- Ver Steeg, Greg and Galstyan, Aram. Maximally informative hierarchical representations of high-dimensional data. In *Artificial Intelligence and Statistics*, pp. 1004–1012, 2015.
- Watanabe, Satoshi. Information theoretical analysis of multivariate correlation. *IBM Journal of research and development*, 4(1):66–82, 1960.
- Zhao, Shengjia, Song, Jiaming, and Ermon, Stefano. Infovae: Information maximizing variational autoencoders. *arXiv preprint arXiv:1706.02262*, 2017.

Supplementary Materials

A. Mutual Information Gap

A.1 Estimation of $I(z_k; v_k)$

With any inference network $q(z|x)$, we can compute the mutual information $I(z; v)$ by assuming the model $p(v)p(x|v)q(z|x)$. Specifically, we compute this for every pair of latent variable z_j and ground truth factor v_k .

We make the following assumptions:

- The inference distribution $q(z_j|x)$ can be sampled from and is known for all j .
- The generating process $p(n|v_k)$ can be sampled from and is known.
- Simplifying assumption: $p(v_k)$ and $p(n|v_k)$ are quantized (ie. the empirical distributions).

We use the following notation:

- Let \mathcal{X}_{v_k} be the support of $p(n|v_k)$.

Then the mutual information can be estimated as following:

$$\begin{aligned}
 & I(z_j; v_k) \\
 &= \mathbb{E}_{q(z_j, v_k)} [\log q(z_j, v_k) - \log q(z_j) - \log p(v_k)] \\
 &= \mathbb{E}_{q(z_j, v_k)} \left[\log \sum_{n=1}^N q(z_j, v_k, n) - \log q(z_j) - \log p(v_k) \right] \\
 &= \mathbb{E}_{p(v_k)p(n'|v_k)q(z_j|n')} \left[\log \sum_{n=1}^N p(v_k)p(n|v_k)q(z_j|n) - \log q(z_j) - \log p(v_k) \right] \tag{S1} \\
 &= \mathbb{E}_{p(v_k)p(n'|v_k)q(z_j|n')} \left[\log \sum_{n=1}^N \mathbb{1}[n \in \mathcal{X}_{v_k}]p(n|v_k)q(z_j|n) \right] + \mathbb{E}_{q(z_j)} [-\log q(z_j)] \\
 &= \mathbb{E}_{p(v_k)p(n'|v_k)q(z_j|n')} \left[\log \sum_{n \in \mathcal{X}_{v_k}} q(z_j|n)p(n|v_k) \right] + H(z_j)
 \end{aligned}$$

where the expectation is to make sampling explicit.

To reduce variance, we perform stratified sampling over $p(v_k)$, and use 10,000 samples from $q(n, z_k)$ for each value of v_k . To estimate $H(z_j)$ we sample from $p(n)q(z_j|n)$ and perform stratified sampling over $p(n)$. The computation time of our estimation procedure depends on the dataset size but in general can be done in a few minutes for the datasets in our experiments.

A.2 Normalization

It is known that when v_k is discrete, then

$$I(z_j; v_k) = \underbrace{H(v_k)}_{\geq 0} - \underbrace{H(v_k|z_j)}_{\geq 0} \leq H(v_k) \tag{S2}$$

This bound is tight if the model can make $H(v_k|z_j)$ zero, ie. there exist an invertible function between z_j and v_k . On the other hand, if mutual information is not maximal, then we know it is because of a high conditional entropy $H(v_k|z_j)$. This suggests our metric is meaningful as it is measuring how much information z_j retains about v_k regardless of the parameterization of their distributions.

B. ELBO TC-Decomposition

Proof of the decomposition in (3):

$$\begin{aligned}
 & \frac{1}{N} \sum_{n=1}^N \mathbf{D}_{\text{KL}}(q(z|x_n)||p(z)) = \mathbb{E}_{p(n)} \left[\mathbf{D}_{\text{KL}}(q(z|n)||p(z)) \right] \\
 &= \mathbb{E}_{p(n)} \left[\mathbb{E}_{q(z|n)} \left[\log q(z|n) - \log p(z) + \log q(z) - \log q(z) + \log \prod_j q(z_j) - \log \prod_j q(z_j) \right] \right] \\
 &= \mathbb{E}_{q(z,n)} \left[\log \frac{q(z|n)}{q(z)} \right] + \mathbb{E}_{q(z)} \left[\log \frac{q(z)}{\prod_j q(z_j)} \right] + \mathbb{E}_{q(z)} \left[\sum_j \log \frac{q(z_j)}{p(z_j)} \right] \\
 &= \mathbb{E}_{q(z,n)} \left[\log \frac{q(z|n)p(n)}{q(z)p(n)} \right] + \mathbb{E}_{q(z)} \left[\log \frac{q(z)}{\prod_j q(z_j)} \right] + \sum_j \mathbb{E}_{q(z)} \left[\log \frac{q(z_j)}{p(z_j)} \right] \\
 &= \mathbb{E}_{q(z,n)} \left[\log \frac{q(z|n)p(n)}{q(z)p(n)} \right] + \mathbb{E}_{q(z)} \left[\log \frac{q(z)}{\prod_j q(z_j)} \right] + \sum_j \mathbb{E}_{q(z_j)q(z_{\setminus j}|z_j)} \left[\log \frac{q(z_j)}{p(z_j)} \right] \\
 &= \mathbb{E}_{q(z,n)} \left[\log \frac{q(z|n)p(n)}{q(z)p(n)} \right] + \mathbb{E}_{q(z)} \left[\log \frac{q(z)}{\prod_j q(z_j)} \right] + \sum_j \mathbb{E}_{q(z_j)} \left[\log \frac{q(z_j)}{p(z_j)} \right] \\
 &= \underbrace{\mathbf{D}_{\text{KL}}(q(z,n)||q(z)p(n))}_{\text{(i) Index-Code MI}} + \underbrace{\mathbf{D}_{\text{KL}}(q(z)||\prod_j q(z_j))}_{\text{(ii) Total Correlation}} + \underbrace{\sum_j \mathbf{D}_{\text{KL}}(q(z_j)||p(z_j))}_{\text{(iii) Dimension-wise KL}}
 \end{aligned}$$

B.1 Minibatch Importance Sampling

First, let $\mathcal{B}_M = \{n_1, \dots, n_M\}$ be a minibatch of M indices where each element is sampled i.i.d. from $p(n)$, so for any sampled batch instance \mathcal{B}_M , $p(\mathcal{B}_M) = (1/N)^M$. Let $r(\mathcal{B}_M|n)$ denote the probability of a sampled minibatch where one of the elements is fixed to be n and the rest are sampled i.i.d. from $p(n)$. This gives $r(x_M|n) = (1/N)^{M-1}$.

$$\begin{aligned}
 & \mathbb{E}_{q(z)} [\log q(z)] \\
 &= \mathbb{E}_{q(z,n)} [\log \mathbb{E}_{n' \sim p(n)} [q(z|n')]] \\
 &= \mathbb{E}_{q(z,n)} \left[\log \mathbb{E}_{p(\mathcal{B}_M)} \left[\frac{1}{M} \sum_{m=1}^M q(z|n_m) \right] \right] \\
 &= \mathbb{E}_{q(z,n)} \left[\log \mathbb{E}_{r(\mathcal{B}_M|n)} \left[\frac{p(\mathcal{B}_M)}{r(\mathcal{B}_M|n)} \frac{1}{M} \sum_{m=1}^M q(z|n_m) \right] \right] \\
 &= \mathbb{E}_{q(z,n)} \left[\log \mathbb{E}_{r(\mathcal{B}_M|n)} \left[\frac{1}{NM} \sum_{m=1}^M q(z|n_m) \right] \right]
 \end{aligned} \tag{S3}$$

During training, when provided with a minibatch of samples $\{n_1, \dots, n_M\}$, we can use the estimator

$$\mathbb{E}_{q(z)} [\log q(z)] \approx \frac{1}{M} \sum_{i=1}^M \left[\log \sum_{j=1}^M q(z(n_i)|n_j) - \log(NM) \right] \tag{S4}$$

where $z(n_i)$ is a sample from $q(z|n_i)$.

C. Factorial Normalizing Flow

We also performed experiments with a factorial normalizing flow (FNF) as a flexible prior. Each dimension is a normalizing flow of depth 32, and the parameters are trained to maximize the β -TCVAE objective. The FNF can fit multi-modal distributions. From our preliminary experiments, we found no significant improvement from using a factorial Gaussian prior and so decided not to include this in the paper.

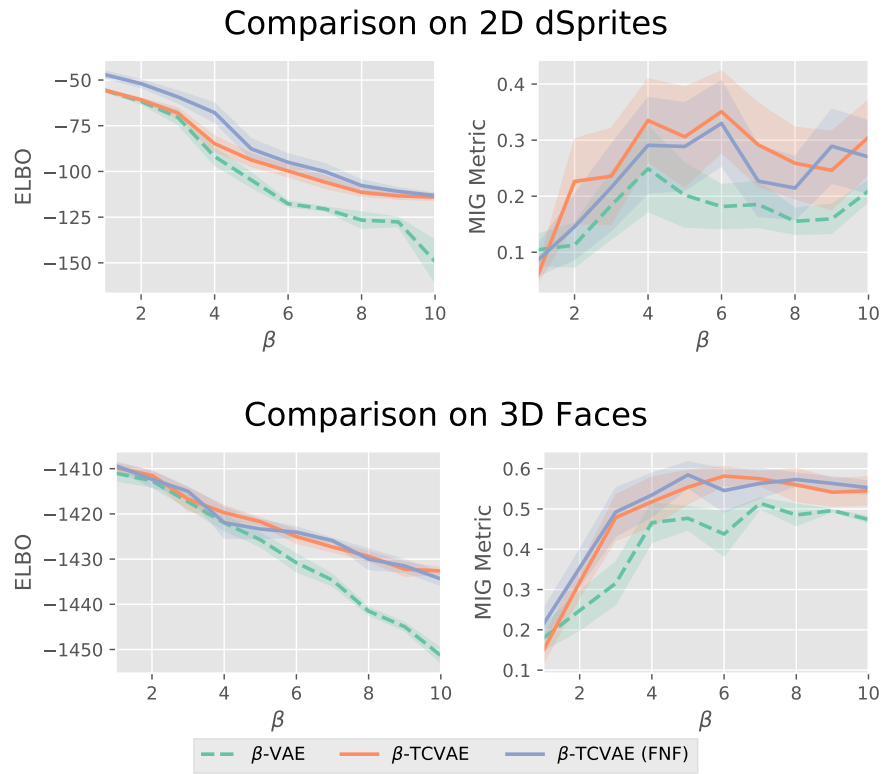


Figure S1. ELBO vs. Disentanglement plots showing the β -TCVAE with a factorial normalizing flow (FNF).

D. Comparison of Best Models

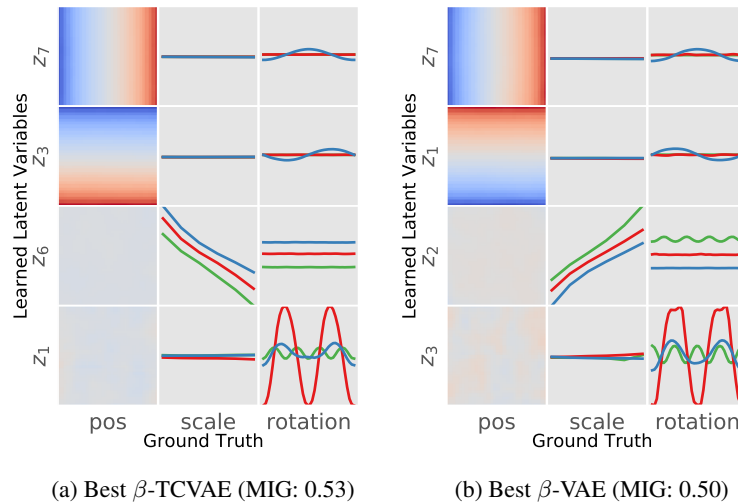


Figure S2. **MIG is able to capture subtle differences.** Relation between the learned variables and the ground truth factors are plotted for the best β -TCVAE and β -VAE on the dSprites dataset according to the MIG metric are shown. Each row corresponds to a ground truth factor and each column to a latent variable. The plots show the relationship between the latent variable mean versus the ground truth factor, with only active latent variables shown. For position, a color of blue indicates a high value and red indicates a low value. The colored lines indicate object shape with red being oval, green being square, and blue being heart. Interestingly, the latent variables for rotation has 2 peaks for oval and 4 peaks for square, suggesting that the models have produced a more compact code by observing that the object is rendered the same for certain degrees of rotation.

E. Invariance to Hyperparameters

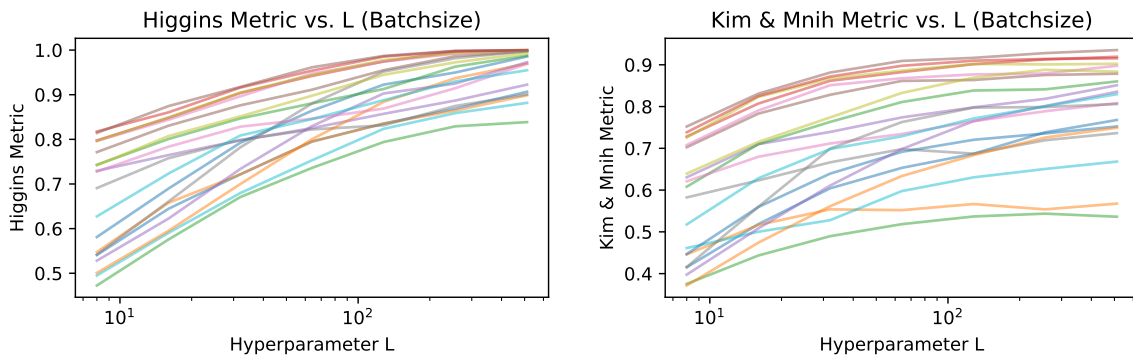


Figure S3. The distribution of each classifier-based metric is shown to be extremely dependent on the hyperparameter L . Each colored line is a different VAE trained with the unmodified ELBO objective.

We believe that a metric should also be invariant to any hyperparameters. For instance, the existence of hyperparameters in the prior metrics means that a different set of hyperparameter values can result in different metric outputs. Additionally, even with a stable classifier that always outputs the same accuracy for a given dataset, the creation of a dataset for classifier-based metrics can still be problematic.

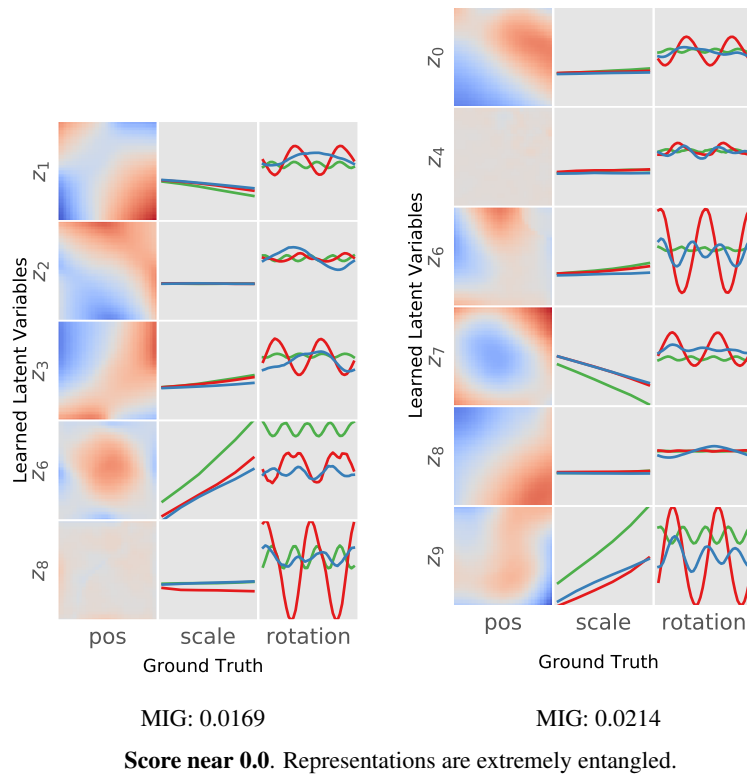
The aggregated inputs used by [Higgins et al. \(2017\)](#) and [Kim & Mnih \(2017\)](#) depend on a batch size L that is difficult to tune and leads to inconsistent metric values. In fact, we empirically find that these metrics are most informative with a small

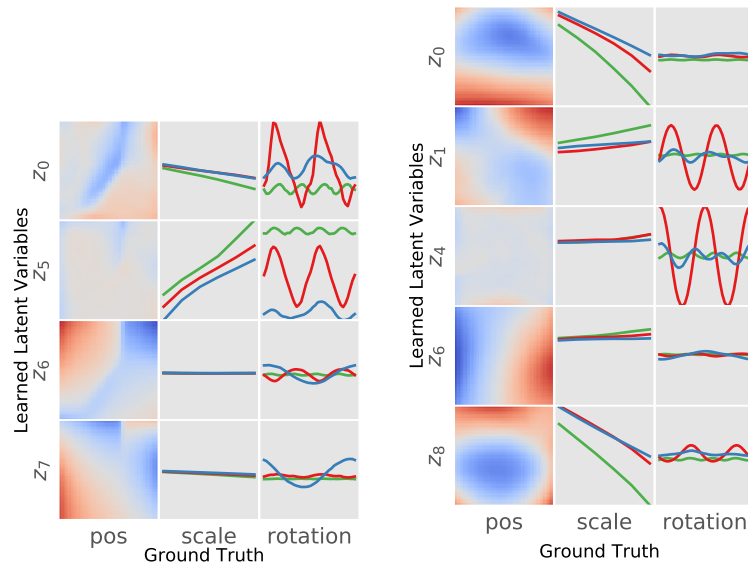
L. Figure S3 plots the Higgins et al. (2017) metric against *L* for 20 fully trained VAEs. As *L* increases, the aggregated inputs become more quantized. Not only does this increase the accuracy of the metric, but it also *reduces the gap between models*, making it hard to discriminate similarly performing models. The relative ordering of models is also not preserved with different values.

F. MIG Traversal

To give some insight into what MIG is capturing, we show some β -TCVAE experiments with scores near quantized values of MIG. In general, we find that MIG gives low scores to entangled representations when even just two variables are not axis-aligned. We find that MIG shows a clearer pattern for scoring position and scale, but less so for rotation. This is likely due to latent variables having a low MI with rotation. In an unsupervised setting, a ground truth rotation of 0 and 180 are impossible to differentiate between for ovals and squares, so the latent variable simply learns to map these to the same value. This is evident in the plots where latent variables describing rotation are many-to-one. The existence of factors with redundant values may be one downside to using MIG as a scoring mechanism, but such factors only appear in simple datasets such as dSprites.

Note that this type of plot does not show the whole picture. Specifically, only the mean of the latent variables is shown, while the uncertainty of the latent variables is not. Mutual information computes the reduction in uncertainty after observing one factor, so the uncertainty is important but cannot be easily plotted. Some changes in MIG may be explained by a reduction in the uncertainty even though the plots may look similar.

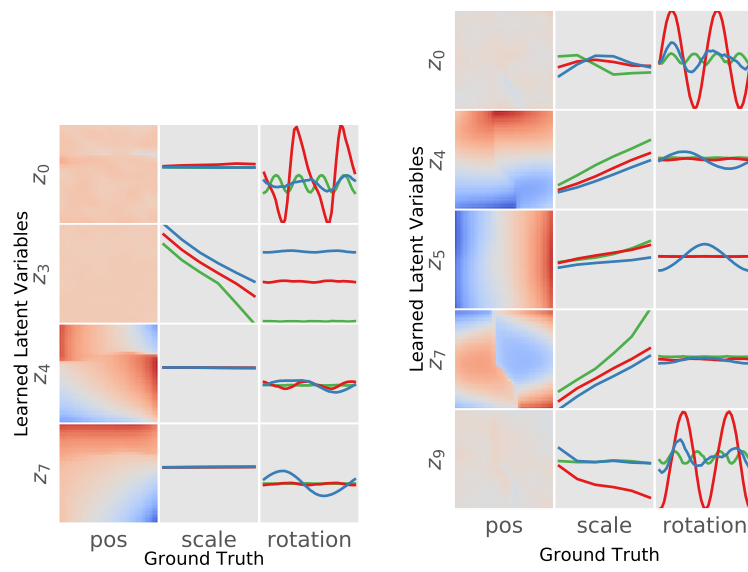




MIG: 0.0988

MIG: 0.1017

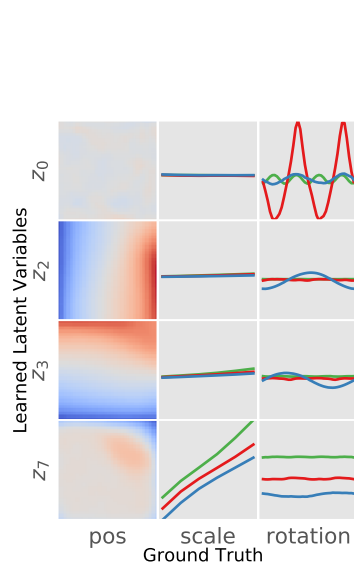
Score near 0.1. Representations are less entangled but fail to satisfy axis-alignment.



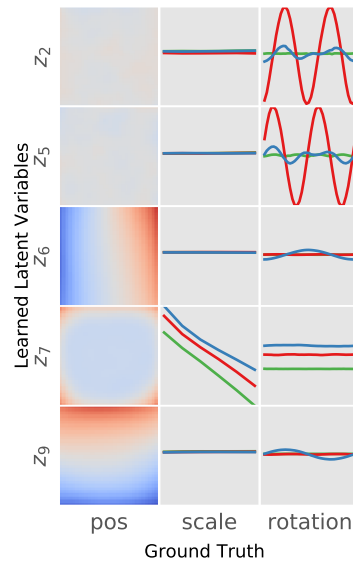
MIG: 0.2017

MIG: 0.2029

Score near 0.2. Representations are still entangled, but some form is appearing.

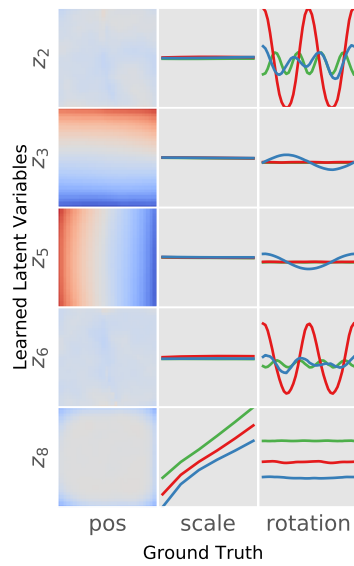


MIG: 0.3155

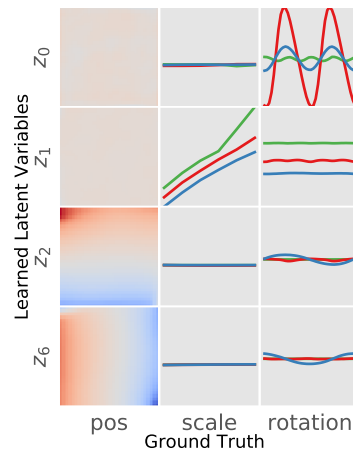


MIG: 0.3271

Score near 0.3. Representations look much more disentangled, with some nuances not being completely disentangled.

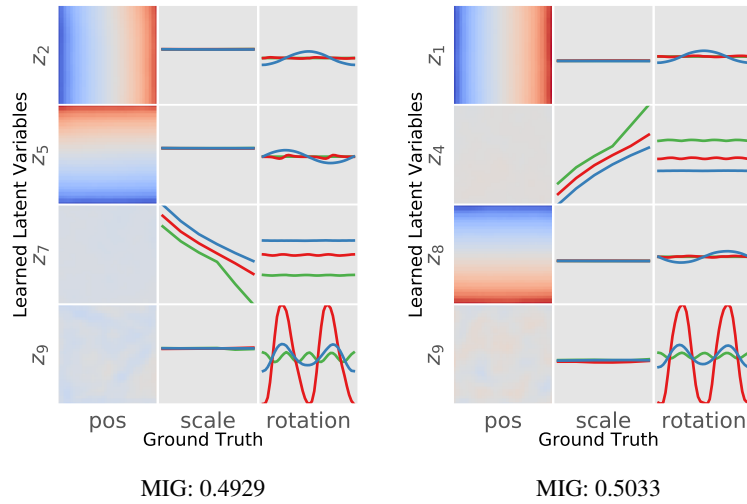


MIG: 0.4092



MIG: 0.4179

Score near 0.4. Representations appear to be axis-aligned but rotation is still entangled.



Score near 0.5. Representations appear to be axis-aligned and disentangled. Higher scores are likely reducing entropy (with latent variables appearing closer to a Dirac delta.) To fully match the ground truth, the latent variables would have to be a mixture of Dirac deltas, which would have a high dimension-wise KL with a factorized Gaussian.

G. Disagreements Between Metrics

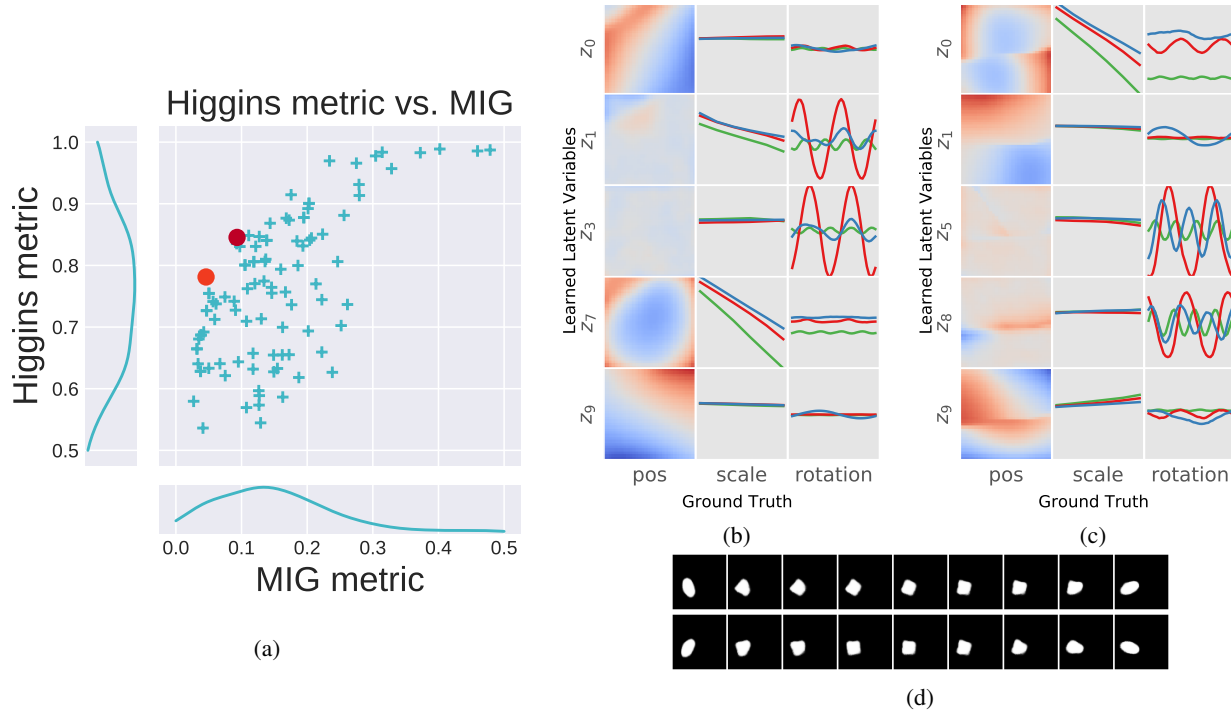


Figure S10. Entangled representations can have a relatively high Higgins metric while MIG correctly scores it low. (a) The Higgins metric tends to be overly optimistic compared to the MIG metric. (b, c) Relationships between the ground truth factors and the learned latent variables are shown for the top two controversial models, which are shown as red dots. Each colored line indicates a different shape (see Supplementary Materials). (d) Sample traversals for the two latent variables in model (b) that both depend on rotation, which clearly mirror each other.

Before using the MIG metric, we first show that it is in some ways superior to the Higgins et al. (2017) metric. To find differences between these two metrics, we train 200 models of β -VAE with varying β and different initializations.

Figure S10a shows each model as a single point based on the two metrics. In general, both metrics agree on the most disentangled models; however, the MIG metric falls off very quickly comparatively. In fact, the Higgins metric tends to output an inflated score due to its inability to detect subtle differences and a lack of axis-alignment.

As an example, we can look at controversial models that are disagreed upon by the two metrics (Figure S10b). The most controversial model is shown in Figure S10a as a red dot. While the MIG metric only ranks this model as better than 26% of the models, the Higgins metric ranks it as better than 75% of the models. By inspecting the relationship between the latent units and ground truth factors, we see that only the scale factor seems to be disentangled (Figure S10b). The position factors are not axis aligned, and there are two latent variables for rotation that appear to mirror each other with only a very slight difference. The two rows in Figure S10d show traversals corresponding to the two latent variables for rotation. We see clearly that they simply rotate in the opposite direction. Since the Higgins metric does not enforce that only a single latent variable should influence each factor, it mistakenly assigns a higher disentanglement score to this model. We note that many models near the black dot in the figure exhibit similar behavior.

G.1 More Controversial Models

Each model can be ordered by either metric (MIG or Higgins) such that each model is assigned a unique integer 1 – 200. We define the most controversial model as $\max_{\alpha} R(\alpha; Higgins) - R(\alpha; MIG)$, where a higher rank implies more disentanglement. These are models that the Higgins metric believes to be highly disentangled while MIG believes they are not. Figure S12 shows the top 5 most controversial models.

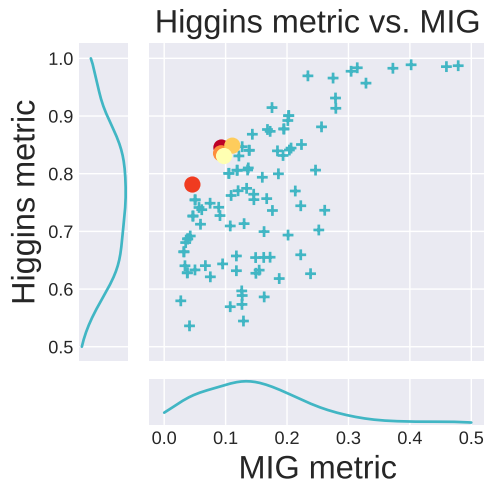


Figure S11. Models as colored dots are those shown in Figure S12.


```

        nn.Linear(input_dim, 1200),
        nn.Tanh(),
        nn.Linear(1200, 1200),
        nn.Tanh(),
        nn.Linear(1200, 1200),
        nn.Tanh(),
        nn.Linear(1200, 4096)
    )

    def forward(self, z):
        h = z.view(z.size(0), -1)
        h = self.net(h)
        mu_img = h.view(z.size(0), 1, 64, 64)
        return mu_img

```

3D Faces and 3D Chairs (except InfoGAN)

```

class ConvEncoder(nn.Module):
    def __init__(self, output_dim):
        super(ConvEncoder, self).__init__()
        self.output_dim = output_dim
        self.conv1 = nn.Conv2d(1, 32, 4, 2, 1) # 32 x 32
        self.bn1 = nn.BatchNorm2d(32)
        self.conv2 = nn.Conv2d(32, 32, 4, 2, 1) # 16 x 16
        self.bn2 = nn.BatchNorm2d(32)
        self.conv3 = nn.Conv2d(32, 64, 4, 2, 1) # 8 x 8
        self.bn3 = nn.BatchNorm2d(64)
        self.conv4 = nn.Conv2d(64, 64, 4, 2, 1) # 4 x 4
        self.bn4 = nn.BatchNorm2d(64)
        self.conv5 = nn.Conv2d(64, 512, 4)
        self.bn5 = nn.BatchNorm2d(512)
        self.conv_z = nn.Conv2d(512, output_dim, 1)
        self.act = nn.ReLU(inplace=True)

    def forward(self, x):
        h = x.view(-1, 1, 64, 64)
        h = self.act(self.bn1(self.conv1(h)))
        h = self.act(self.bn2(self.conv2(h)))
        h = self.act(self.bn3(self.conv3(h)))
        h = self.act(self.bn4(self.conv4(h)))
        h = self.act(self.bn5(self.conv5(h)))
        z = self.conv_z(h).view(x.size(0), self.output_dim)
        return z

class ConvDecoder(nn.Module):
    def __init__(self, input_dim):
        super(ConvDecoder, self).__init__()
        self.conv1 = nn.ConvTranspose2d(input_dim, 512, 1, 1, 0) # 1 x 1
        self.bn1 = nn.BatchNorm2d(512)
        self.conv2 = nn.ConvTranspose2d(512, 64, 4, 1, 0) # 4 x 4
        self.bn2 = nn.BatchNorm2d(64)
        self.conv3 = nn.ConvTranspose2d(64, 64, 4, 2, 1) # 8 x 8
        self.bn3 = nn.BatchNorm2d(64)
        self.conv4 = nn.ConvTranspose2d(64, 32, 4, 2, 1) # 16 x 16

```

```

self.bn4 = nn.BatchNorm2d(32)
self.conv5 = nn.ConvTranspose2d(32, 32, 4, 2, 1) # 32 x 32
self.bn5 = nn.BatchNorm2d(32)
self.conv_final = nn.ConvTranspose2d(32, 1, 4, 2, 1)
self.act = nn.ReLU(inplace=True)

def forward(self, z):
    h = z.view(z.size(0), z.size(1), 1, 1)
    h = self.act(self.bn1(self.conv1(h)))
    h = self.act(self.bn2(self.conv2(h)))
    h = self.act(self.bn3(self.conv3(h)))
    h = self.act(self.bn4(self.conv4(h)))
    h = self.act(self.bn5(self.conv5(h)))
    mu_img = self.conv_final(h)
    return mu_img

```

InfoGAN

```

class ConvEncoder(nn.Module):
    def __init__(self, output_dim):
        super(ConvEncoder, self).__init__()
        self.output_dim = output_dim

        self.conv1 = nn.Conv2d(1, 32, 4, 2, 1) # 32 x 32
        self.bn1 = nn.BatchNorm2d(32)
        self.conv2 = nn.Conv2d(32, 32, 4, 2, 1) # 16 x 16
        self.bn2 = nn.BatchNorm2d(32)
        self.conv3 = nn.Conv2d(32, 64, 4, 2, 1) # 8 x 8
        self.bn3 = nn.BatchNorm2d(64)
        self.conv4 = nn.Conv2d(64, 64, 4, 2, 1) # 4 x 4
        self.bn4 = nn.BatchNorm2d(64)
        self.conv5 = nn.Conv2d(64, 512, 4)
        self.bn5 = nn.BatchNorm2d(512)
        self.conv_z = nn.Conv2d(512, output_dim, 1)
        self.conv_d = nn.Conv2d(512, 1, 1)
        self.act = nn.LeakyReLU(0.2, inplace=True)

    def forward(self, x):
        return self.recognition(x)

    def discriminate(self, x):
        h = x.view(-1, 1, 64, 64)
        h = self.act(self.bn1(self.conv1(h)))
        h = self.act(self.bn2(self.conv2(h)))
        h = self.act(self.bn3(self.conv3(h)))
        h = self.act(self.bn4(self.conv4(h)))
        h = self.act(self.bn5(self.conv5(h)))
        d = self.conv_d(h).view(x.size(0), 1)
        return d

    def recognition(self, x):
        h = x.view(-1, 1, 64, 64)
        h = self.act(self.bn1(self.conv1(h)))
        h = self.act(self.bn2(self.conv2(h)))

```

```

h = self.act(self.bn3(self.conv3(h)))
h = self.act(self.bn4(self.conv4(h)))
h = self.act(self.bn5(self.conv5(h)))
z = self.conv_z(h).view(x.size(0), self.output_dim)
return z

```

```

class ConvDecoder(nn.Module):
    def __init__(self, input_dim):
        super(ConvDecoder, self).__init__()
        self.conv1 = nn.ConvTranspose2d(input_dim, 512, 1, 1, 0) # 1 x 1
        self.bn1 = nn.BatchNorm2d(512)
        self.conv2 = nn.ConvTranspose2d(512, 64, 4, 1, 0) # 4 x 4
        self.bn2 = nn.BatchNorm2d(64)
        self.conv3 = nn.ConvTranspose2d(64, 64, 4, 2, 1) # 8 x 8
        self.bn3 = nn.BatchNorm2d(64)
        self.conv4 = nn.ConvTranspose2d(64, 32, 4, 2, 1) # 16 x 16
        self.bn4 = nn.BatchNorm2d(32)
        self.conv5 = nn.ConvTranspose2d(32, 32, 4, 2, 1) # 32 x 32
        self.bn5 = nn.BatchNorm2d(32)
        self.conv_final = nn.ConvTranspose2d(32, 1, 4, 2, 1)
        self.act = nn.LeakyReLU(0.2, inplace=True)

    def forward(self, z):
        h = z.view(z.size(0), z.size(1), 1, 1)
        h = self.act(self.bn1(self.conv1(h)))
        h = self.act(self.bn2(self.conv2(h)))
        h = self.act(self.bn3(self.conv3(h)))
        h = self.act(self.bn4(self.conv4(h)))
        h = self.act(self.bn5(self.conv5(h)))
        mu_img = self.conv_final(h)
        return mu_img

```

CelebA

```

class ConvEncoder(nn.Module):
    def __init__(self, output_dim):
        super(ConvEncoder, self).__init__()
        self.output_dim = output_dim
        self.conv1 = nn.Conv2d(3, 64, 4, 2, 1) # 32 x 32
        self.bn1 = nn.BatchNorm2d(64)
        self.conv2 = nn.Conv2d(64, 128, 4, 2, 1) # 16 x 16
        self.bn2 = nn.BatchNorm2d(128)
        self.conv3 = nn.Conv2d(128, 128, 4, 2, 1) # 8 x 8
        self.bn3 = nn.BatchNorm2d(128)
        self.conv4 = nn.Conv2d(128, 256, 4, 2, 1) # 4 x 4
        self.bn4 = nn.BatchNorm2d(256)
        self.conv5 = nn.Conv2d(256, 512, 4)
        self.bn5 = nn.BatchNorm2d(512)
        self.conv_z = nn.Conv2d(512, output_dim, 1)
        self.act = nn.ReLU(inplace=True)

    def forward(self, x):

```

Isolating Sources of Disentanglement in Variational Autoencoders

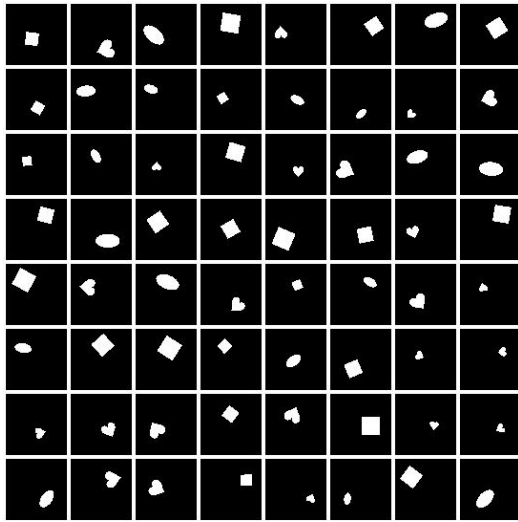
```
h = x.view(-1, 3, IMG_SIZE, IMG_SIZE)
h = self.act(self.bn1(self.conv1(h)))
h = self.act(self.bn2(self.conv2(h)))
h = self.act(self.bn3(self.conv3(h)))
h = self.act(self.bn4(self.conv4(h)))
h = self.act(self.bn5(self.conv5(h)))
z = self.conv_z(h).view(x.size(0), self.output_dim)
return z

class ConvDecoder(nn.Module):
    def __init__(self, input_dim):
        super(ConvDecoder, self).__init__()
        self.conv1 = nn.ConvTranspose2d(input_dim, 512, 1, 1, 0) # 1 x 1
        self.bn1 = nn.BatchNorm2d(512)
        self.conv2 = nn.ConvTranspose2d(512, 256, 4, 1, 0) # 4 x 4
        self.bn2 = nn.BatchNorm2d(256)
        self.conv3 = nn.ConvTranspose2d(256, 128, 4, 2, 1) # 8 x 8
        self.bn3 = nn.BatchNorm2d(128)
        self.conv4 = nn.ConvTranspose2d(128, 128, 4, 2, 1) # 16 x 16
        self.bn4 = nn.BatchNorm2d(128)
        self.conv5 = nn.ConvTranspose2d(128, 64, 4, 2, 1) # 32 x 32
        self.bn5 = nn.BatchNorm2d(64)
        self.conv_final_mu = nn.ConvTranspose2d(64, 3, 4, 2, 1)
        self.act = nn.ReLU(inplace=True)

    def forward(self, z):
        batchsize = z.size(0)
        h = z.view(batchsize, -1, 1, 1)
        h = self.act(self.bn1(self.conv1(h)))
        h = self.act(self.bn2(self.conv2(h)))
        h = self.act(self.bn3(self.conv3(h)))
        h = self.act(self.bn4(self.conv4(h)))
        h = self.act(self.bn5(self.conv5(h)))
        img_mu = self.conv_final_mu(h).view(batchsize, 3, 64, 64).sigmoid()
        return img_mu
```

I. Random Samples

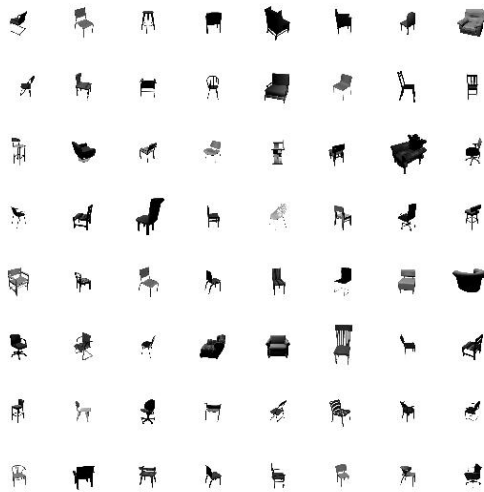
I.1 Real Samples



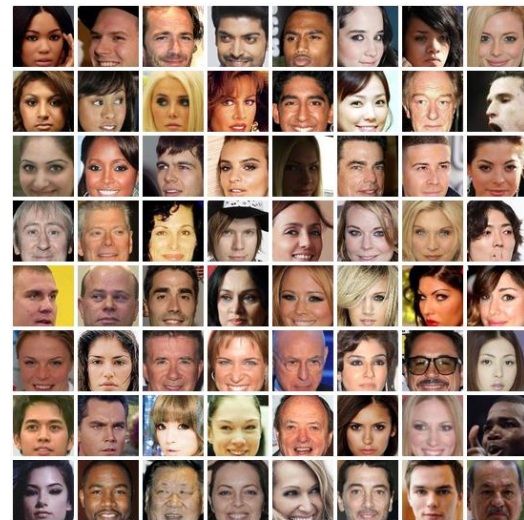
dSprites (64×64)



3D Faces (64×64)



3D Chairs (64×64)



CelebA (64×64)

Figure S13. Real samples from the training data set.

I.2 Latent Traversals

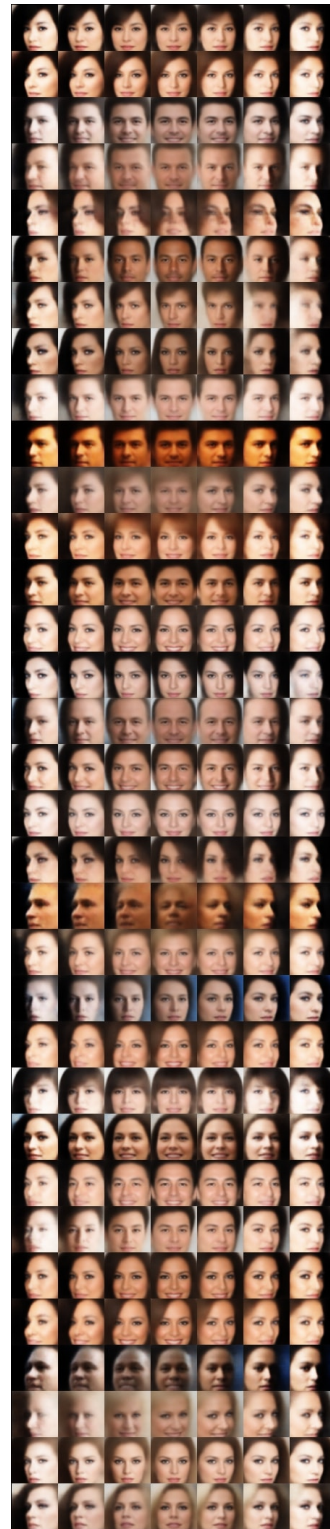
β -TCVAE MODEL ONE ($\beta=15$)



Baldness

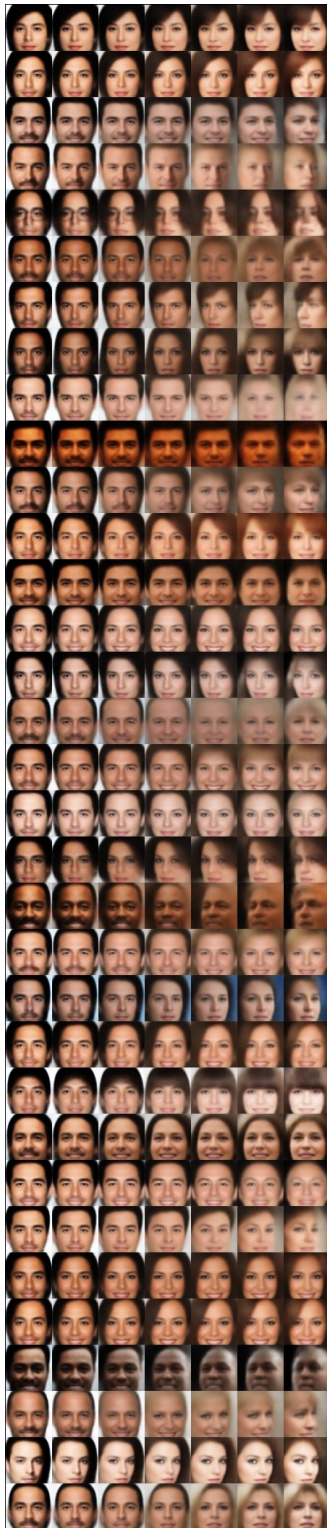


Dramatic masculinity

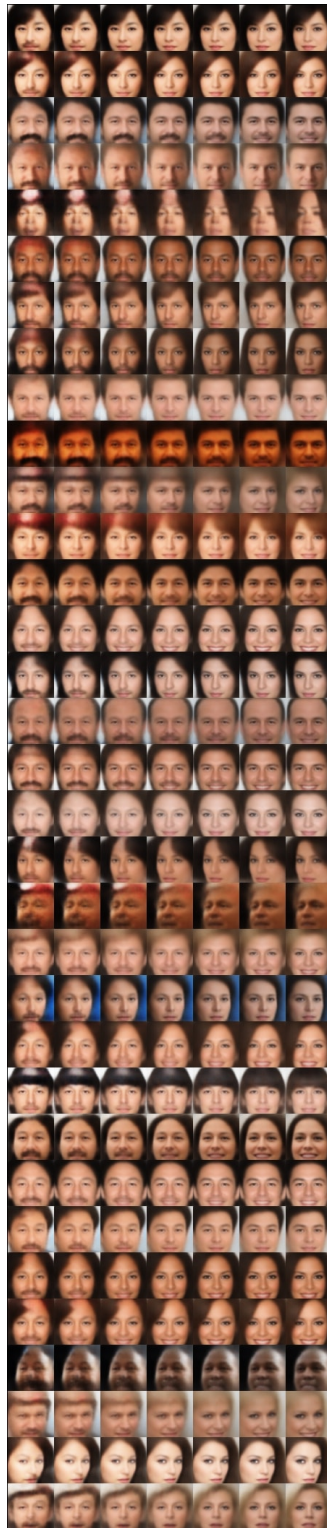


Azimuth

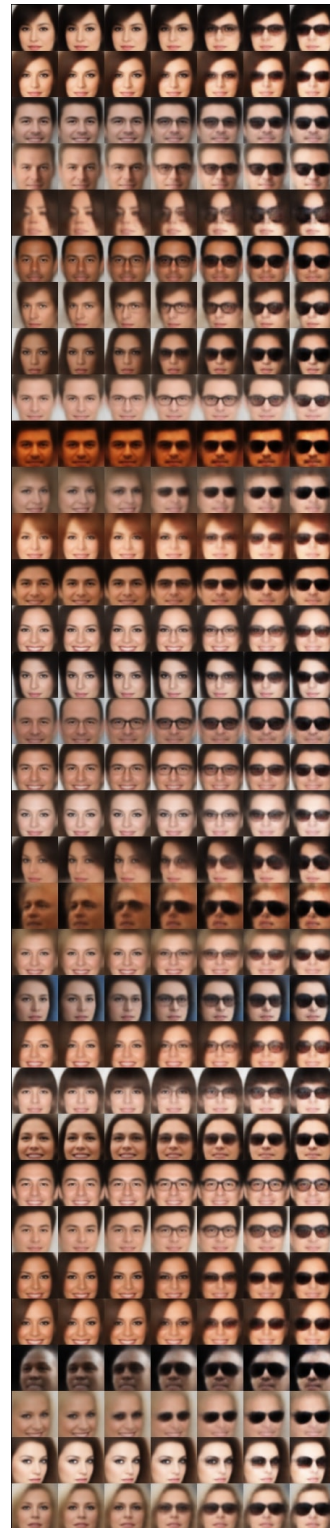
Isolating Sources of Disentanglement in Variational Autoencoders



Contrast

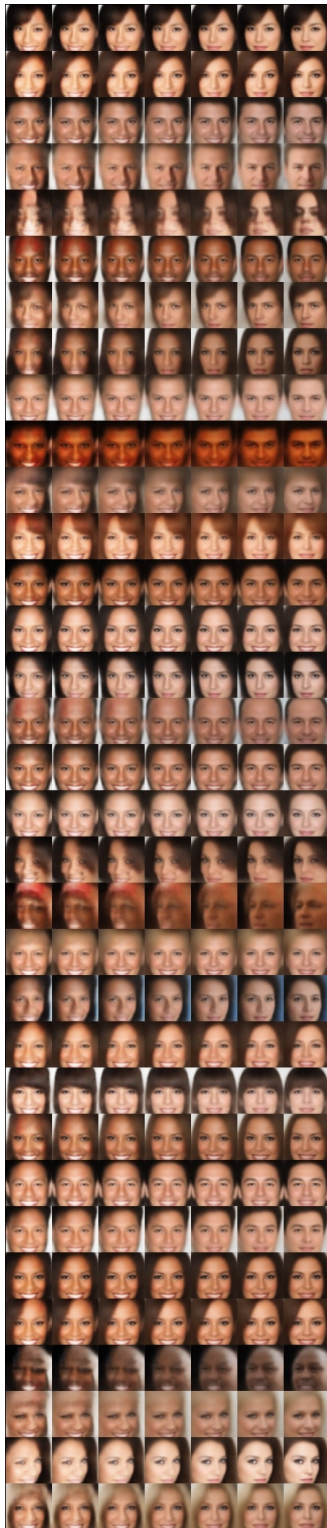


Mustache (shared with Glasses)

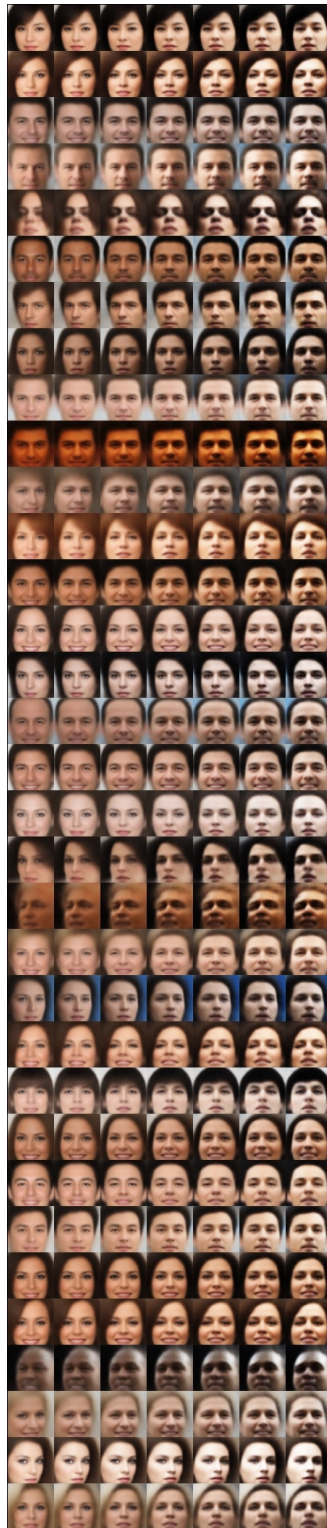


Glasses (shared with Mustache)

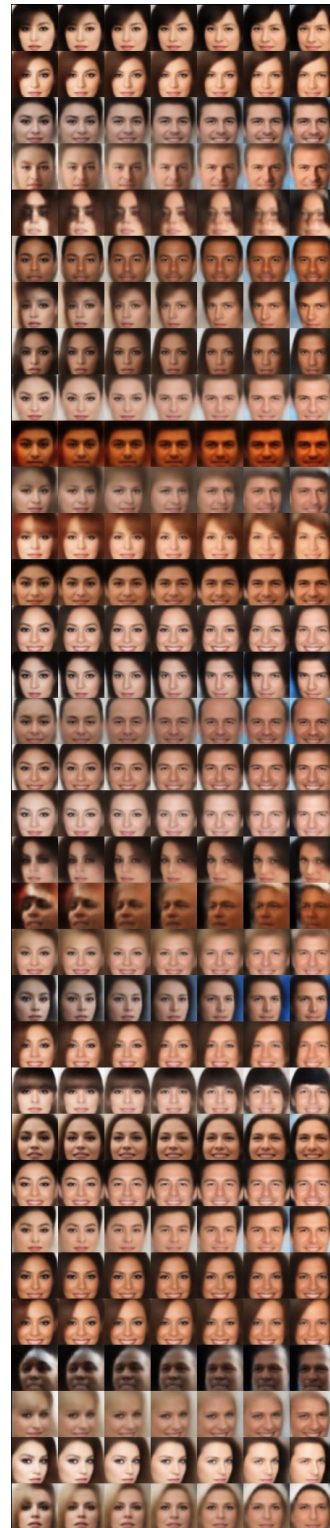
Isolating Sources of Disentanglement in Variational Autoencoders



Smile (shared with Shadow)



Shadow (shared with Smile)



Gender

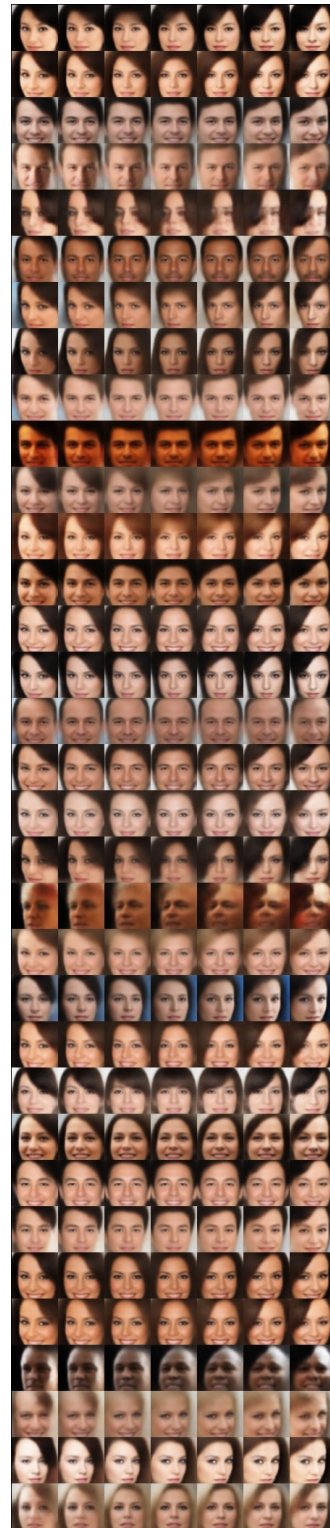
Isolating Sources of Disentanglement in Variational Autoencoders



Skin color



Brightness

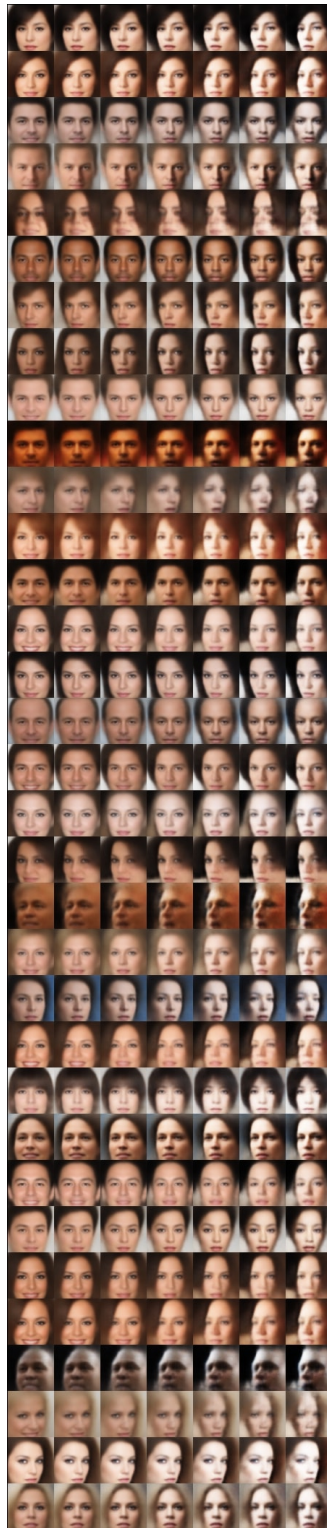


Bangs (side)

Isolating Sources of Disentanglement in Variational Autoencoders



Hue



Face width



Eye shadow